Picosecond Carrier Lifetime in Low-Temperature-Grown GaAsSb

Xavier Wallart*, Christophe Coinon, Sébastien Plissard, Sylvie Godey, Olivier Offranc, Ydir Androussi[1], Vincent Magnin, and Jean-François Lampin

Institut d'Electronique, de Microélectronique et de Nanotechnologie, UMR CNRS 8520, Université de Lille 1, Avenue Poincaré, P. O. Box 60069, 59652 Villeneuve d'Ascq, France
[1]*Unité Matériaux et Transformations, UMR CNRS 8207, Université de Lille 1, 59655 Villeneuve d'Ascq, France*

Received September 29, 2010; accepted October 17, 2010; published online November 5, 2010

We study the influence of growth parameters on the properties of low-temperature-grown GaAsSb layers with 15–20% Sb. We demonstrate that a proper choice of growth conditions allows achieving monocrystalline as-grown layers exhibiting carrier lifetime around 1 ps and a resistivity higher than 1 kΩ·cm. Upon 600 °C annealing, the resistivity strongly decreases, indicating differences with previous observations, which we try to elucidate. The as-grown material properties are promising for THz generation and detection using a wavelength of around 1.05 μm.
© 2010 The Japan Society of Applied Physics

DOI: 10.1143/APEX.3.111202

Low-temperature-grown GaAs (LTG GaAs) has been proven to exhibit unique properties for ultrafast photoconductive devices used in terahertz (THz) generation and detection working around an 800 nm wavelength. However, with the development of compact and cheap laser sources at telecommunication wavelength (1.55 μm) and using ytterbium-based technology near 1.06 μm, photoconductive materials working above 1 μm are highly desirable. Using III–V materials, except nitrides, the main available alloy families compatible with commercially semi-insulating substrates at this wavelength range are the InGaAs and GaAsSb ones. The former has been extensively explored during the last few decades, whereas rather few results are reported concerning the latter.

For the alloy composition lattice-matched to InP, no relevant carrier lifetime and material resistivity have been achieved using as grown LTG-InGaAs materials, and thus, more sophisticated approaches have been developed.[1–9] They have led to picosecond (ps) or even shorter carrier lifetime materials and THz generation. Both generation and detection have even been demonstrated based on Be-compensated InAlAs/InGaAs multiquantum wells.[10,11] Nevertheless, the low resistivity of the resulting layers remains a bottleneck since the highest reported values lie in the 100 Ω·cm–1 kΩ·cm range, far below those commonly measured on LTG-GaAs (10^6–10^7 Ω·cm). This severely reduces the signal-to-noise ratio of THz detectors. Lower Indium compositions corresponding to a 1.05 μm wavelength have also been investigated but to a lesser extent[12–14] and exhibit a resistivity reaching 10 kΩ·cm[12] with a carrier lifetime below 1 ps. Finally, ps lifetime has recently been reported in LTG-GaBiAs.[15,16]

In this context, the GaAsSb alloy family is worth exploring, which is much less considered up to now. Sigmund *et al.* have reported interesting results on this alloy for a 40% Sb composition.[17–20] The alloy has been grown at low temperature on GaAs substrates with an intermediate $In_{0.23}Al_{0.77}As$ layer. The authors have obtained rather high resistivity, around 10 kΩ·cm, on 0.6-μm-thick films and used the resulting material for THz generation.[20] Moreover, they have observed the formation of clusters, mainly at the InAlAs/GaAsSb interface, without a precise description of their chemical nature. Nevertheless, from these results, some questions remain, especially concerning the meaning of the measured resistivity on such thin layers taking into account surface depletion, the carrier lifetime, and the evolution of the material properties with the growth conditions. In the same way, Willer *et al.*[21] have reported THz generation via photomixing using a 19% Sb alloy, but without any details on the material properties.

Here, we study the influence of the growth parameters on the structural, electrical, and optical properties of thick LTG-GaAsSb layers. We focus on alloys with an Sb composition around 15–20%, corresponding to a working wavelength around 1.05 μm.

The samples are grown on 2-in. semi-insulating (001) GaAs substrates by gas-source molecular beam epitaxy (GSMBE) in a Riber 32P chamber. The arsenic flux is obtained by cracking arsine (AsH_3) through a high-temperature injector, producing mainly an As_2 beam, whereas a valve-cracker source is used for Sb, resulting in an Sb_2 beam. As and Sb fluxes are calibrated via group V-element-limited reflection high energy electron diffraction (RHEED) specular beam intensity oscillations on GaAs and GaSb. The growth rate is 1 monolayer/s (ML/s) and the layer thickness is 1.5 μm. To achieve Sb contents of the GaAsSb layers in the 15–20% range, we assume that the sticking coefficient of Sb is greater than the As one and nearly equal to unity. We then choose an equivalent Sb flux of 0.2 ML/s and vary the equivalent As flux between 1 and 2 ML/s. The growth temperature (T_G) is kept in the 250–330 °C range and measured by band-edge absorption spectroscopy allowing temperature measurements down to 300 K. The samples have been characterized before and after a 600 °C, 1 min rapid thermal annealing (RTA) in N_2 atmosphere.

The RHEED observations during growth are summarized in Fig. 1. For growth temperatures below 300 °C, starting with the initial streaky pattern of the GaAs surface, the RHEED diagram transforms quickly into a spotty one, revealing surface roughness. Then, circles begin to appear in the diagram and reinforce until the end of the growth, which are characteristics of polycrystalline material. In contrast, when the growth temperature is higher than 300 °C, the RHEED pattern exhibits a slight "spotty" character with a clearly distinguishable (1×3) reconstruction. The layer is then monocrystalline with a more bi-dimensional growth mode [Fig. 1(a)]. The (1×3) reconstruction is associated with Sb-containing material, typical of GaSb growth. In

*E-mail address: xavier.wallart@iemn.univ-lille1.fr

© 2010 The Japan Society of Applied Physics

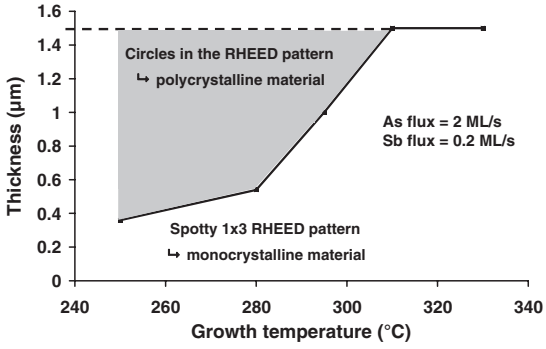

(a)

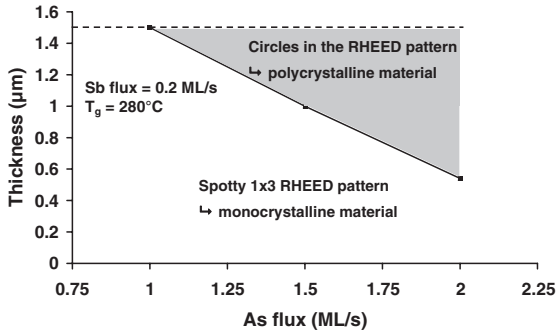

(b)

Fig. 1. Mono- to polycrystalline material transition vs the growth temperature (a) and the As flux (b). The upper dashed line indicates the total layer thickness (1.5 μm).

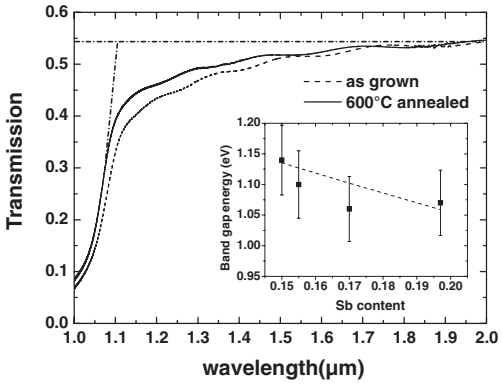

Fig. 2. Optical transmission for a 1.5-μm-thick GaAsSb layer grown at 280 °C with a 1 ML/s As flux, as-grown and after a 600 °C annealing. The straight dashed-dotted lines indicate the bandgap determination. The insert depicts the band gap variation versus Sb content compared to the expected evolution according to eq. (1).

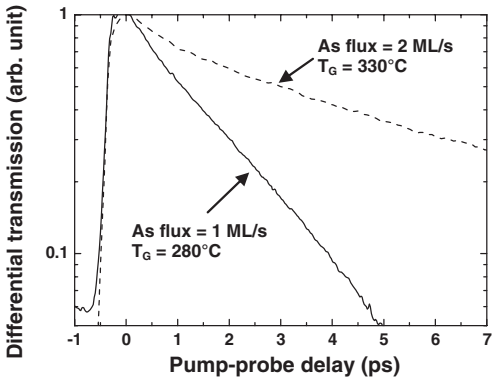

Fig. 3. Time resolved pump-probe measurement at $\lambda = 1.05\,\mu m$ on a 1.5-μm-thick GaAsSb layer grown at 280 °C with a 1 ML/s As flux (solid line) and grown at 330 °C with a 2 ML/s As flux (dashed line).

Fig. 1(b), the growth temperature is kept constant at 280 °C during the entire growth and we have varied the As flux. As can be seen, a high As flux promotes polycrystalline material formation, whereas the layer is fully monocrystalline for the lowest As flux. This monocystalline/polycrystalline transition is confirmed by cross-sectional scanning electron microscopy (SEM) observation (not shown).

For Sb contents between 15 and 20% and a 1.5 μm thickness, the layers are partially plastically relaxed. Triple axis X-ray diffraction (TAXRD) is then used to measure both the layer composition and relaxation by recording reciprocal space maps in the $\langle 110 \rangle$ and $\langle 1\bar{1}0 \rangle$ directions for the symmetric (004) and asymmetric (224) reflections. The deduced composition values are in good agreement with the energy dispersive X-ray fluorescence (EDX) results and no significant composition and relaxation changes have been observed after a 600 °C annealing. For an As flux of 2 ML/s, the layer relaxation increases from a few percent at $T_G = 250$ °C to around 80% for $T_G > 300$ °C. At $T_G = 280$ °C, the relaxation decreases from 75% for a 1 ML/s As flux to 50% for a 2 ML/s one. It clearly demonstrates that the layer relaxation increases with higher growth temperatures and lower As fluxes.

The layer bandgap has been determined by optical absorption, as illustrated in Fig. 2. The bandgap edge is clearly observed together with an Urbach tail and small Fabry–Perot oscillations due to the refractive index difference between GaAs and GaAsSb. For an Sb content between 15 and 20%, we measure bandgap values ranging from 1.05 to 1.15 eV. Assuming a quadratic dependence of the bandgap with the Sb content, the bandgap of the GaAsSb alloy can be determined using the formula:

$$E_g(GaAs_{1-x}Sb_x) = (1-x)\cdot E_g(GaAs) + x\cdot E_g(GaSb) - x\cdot(1-x)\cdot C, \quad (1)$$

where x is the Sb content and C the bowing parameter. Assuming $E_g(GaAs) = 1.422$ eV, $E_g(GaSb) = 0.727$ eV at 300 K, and $C = 1.43$,[22] the calculated values of the bandgap range from 1.05 to 1.16 eV. The agreement between these values and our measured ones is then rather good, reinforcing the overall consistency of our measurements.

Carrier lifetimes are deduced from time-resolved normalized differential transmission, thanks to a pump-probe experiment setup with a periodically poled lithium niobate crystal-based optical parametric oscillator (OPO) pumped by a Ti:sapphire laser (Fig. 3). The evolution of the carrier lifetime with the growth conditions is depicted in Fig. 4. A low carrier lifetime below 1 ps can be obtained, either at low growth temperatures or for high As fluxes, but the related layers are partly polycrystalline. The best trade-off between structural quality and carrier lifetime is obtained for a growth temperature of 280 °C and a low As flux of 1 ML/s. In this case, the carrier lifetime lies slightly above 1 ps before and after a 600 °C annealing.

For monocrystalline samples, the resistivity of the as-grown layers, as given by Hall effect measurements in the van der Pauw configuration, increases from 70 ($T_G = 330$

© 2010 The Japan Society of Applied Physics

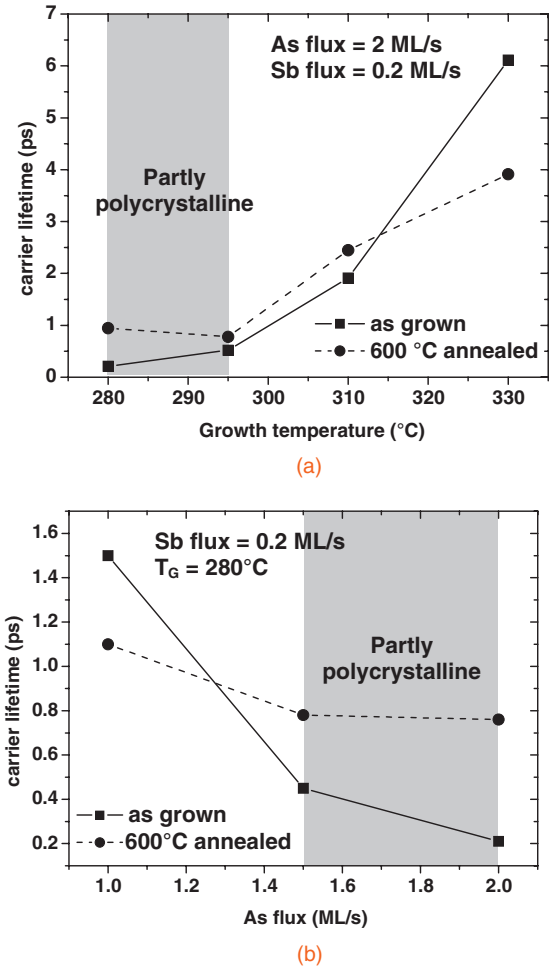

Fig. 4. Evolution of the carrier lifetime vs the growth temperature (a) and the As flux (b) for as-grown and 600 °C-annealed GaAsSb layers.

°C, As flux = 2 ML/s) to 1350 Ω·cm (T_G = 280 °C, As flux = 1 ML/s). The residual carrier concentration is n-type in the 10^{12}–10^{13}/cm^3 range and the corresponding mobility varies from 300 to 1800 cm^2·V^{-1}·s^{-1}. A 600 °C annealing always results in an important drop of the resistivity, mainly due to an increase of the residual carrier concentration (a few 10^{14}/cm^3). As an example, the resistivity of the most resistive as-grown sample decreases from 1350 to 25 Ω·cm.

The above results demonstrate that a careful choice of growth conditions allows achieving picosecond carrier lifetime in LTG-GaAsSb with a rather high resistivity of the as-grown layers. The latter is comparable to the highest values reported either for LTG-InGaAs or LTG-GaAsSb. Nevertheless, the resistivity drop after a 600 °C annealing differs markedly with previous results on these alloys as well as with the standard behavior of LTG-GaAs. For LTG-GaAs, it is well documented that the as-grown material is nonstoichiometric with an excess of arsenic atoms occupying interstitial, antisite positions and also involved in more complex point defects.[12] Upon annealing, this excess arsenic agglomerates in clusters which could explain the high material resistivity. In LTG-GaAsSb, Sigmund *et al.* have also reported the existence of clusters after a 600 °C annealing.[18,19] These clusters are observed preferentially at the interface with the AlInAs intermediate layer that they used. The authors link these observations with the strain relaxation occurring during the annealing. In our case, transmission electron microscopy (TEM) observations (not shown) do not reveal any clear evidence of clustering through the entire layer before and after the annealing. Moreover, even if the lattice mismatch between the GaAsSb layers with 15–20% Sb considered here is similar to that between $GaAs_{0.6}Sb_{0.4}$ and $Al_{0.77}In_{0.23}As$ investigated in the work of Sigmund *et al.* (around 1.5%), our TAXRD measurements do not show any clear strain relaxation due to the 600 °C annealing. We then conclude that the mechanisms involved in our layers are different from those described by Sigmund *et al.* In our case, it appears that the annealing, instead of inducing clustering, reduces the density of deep traps and increases the shallow donor one, as evidenced by the increase of the free carrier density. This discrepancy can tentatively be ascribed to the difference in Sb composition of the GaAsSb alloy (15–20% in this work, 40% in the study of Sigmund *et al.*) and to the difference in the nature of the As flux used. Indeed, we used an As_2 flux whereas Sigmund *et al.* used an As_4 flux. They mention critical thickness differences during the growth of their alloys due to the nature of the As flux.[18] The exact influence of the nature of the As flux of the GaAsSb alloy properties clearly requires further investigation.

In conclusion, we have shown that a proper choice of growth conditions allows achieving picosecond carrier lifetime in as-grown LTG-GaAsSb layers with 15–20% Sb, with a resistivity exceeding 1 kΩ·cm. A 600 °C annealing does not improve these values, since it leads to a marked resistivity drop. Higher resistivity values might be obtained thanks to a p-type doping compensation process, using for instance Be. Nevertheless, the characteristics of the as-grown samples are promising for use in THz generation and detection devices.

Acknowledgments This work was carried out with the financial support of the French Direction Générale de l'Armement under contract N° REI N° 07 34 014 and under a grant for one of us (O. Offranc).

1) E. R. Brown *et al.*: Semicond. Sci. Technol. **20** (2005) S199, and references therein.
2) H. Künzel *et al.*: J. Cryst. Growth **227–228** (2001) 284.
3) M. Gicquel-Guezo *et al.*: Appl. Phys. Lett. **85** (2004) 5926.
4) M. Suzuki and M. Tonouchi: Appl. Phys. Lett. **86** (2005) 163504.
5) R. Takahashi *et al.*: Appl. Phys. Lett. **68** (1996) 153.
6) K. Biermann *et al.*: Appl. Phys. Lett. **80** (2002) 1936.
7) M. Martin *et al.*: Appl. Phys. Lett. **95** (2009) 141910.
8) A. Takanazo *et al.*: Appl. Phys. Lett. **90** (2007) 101119.
9) C. D. Wood *et al.*: Appl. Phys. Lett. **96** (2010) 194104.
10) B. Sartorius *et al.*: Opt. Express **16** (2008) 9565.
11) A. Takazato *et al.*: Appl. Phys. Lett. **91** (2007) 011102.
12) S. Gupta *et al.*: J. Quantum Electron. **28** (1992) 2464.
13) C. Baker *et al.*: Appl. Phys. Lett. **83** (2003) 4113.
14) R. Czarny *et al.*: Electron. Lett. **40** (2004) 942.
15) K. Bertulis *et al.*: Appl. Phys. Lett. **88** (2006) 201112.
16) V. Pacebutas *et al.*: Appl. Phys. Lett. **97** (2010) 031111.
17) J. Sigmund and H. L. Hartnagel: J. Cryst. Growth **278** (2005) 209.
18) J. Sigmund *et al.*: Appl. Phys. Lett. **87** (2005) 252103.
19) J. Sigmund *et al.*: J. Vac. Sci. Technol. B **24** (2006) 1556.
20) S. Hargreaves *et al.*: Solid-State Electron. **53** (2009) 160.
21) U. Willer *et al.*: Appl. Phys. B **87** (2007) 13.
22) I. Vurgaftman *et al.*: J. Appl. Phys. **89** (2001) 5815.

© 2010 The Japan Society of Applied Physics